Mesoscopic electronic heterogeneities in the transport properties of V_2O_3 thin films

2008 J. Phys.: Condens. Matter 20 472205

(http://iopscience.iop.org/0953-8984/20/47/472205)

IOP FTC
IOP PUBLISHING JOURNAL OF PHYSICS: CONDENSED MATTER
J. Phys.: Condens. Matter **20** (2008) 472205 (6pp) doi:10.1088/0953-8984/20/47/472205

FAST TRACK COMMUNICATION

Mesoscopic electronic heterogeneities in the transport properties of V_2O_3 thin films

C Grygiel[1], A Pautrat[1], W C Sheets[1], W Prellier[1], B Mercey[1] and L Méchin[2]

[1] Laboratoire CRISMAT, UMR 6508 du CNRS, ENSICAEN et Université de Caen, 6 Boulevard Maréchal Juin, F-14050 Caen 4, France
[2] GREYC, UMR 6072 du CNRS, ENSICAEN et Université de Caen, 6 Boulevard Maréchal Juin, F-14050 Caen 4, France

Received 21 October 2008
Published 6 November 2008
Online at stacks.iop.org/JPhysCM/20/472205

Abstract
The spectacular metal-to-insulator transition of V_2O_3 can be progressively suppressed in thin film samples. Evidence for phase separation was observed using microbridges as a mesoscopic probe of transport properties, where the same film possesses domains that exhibit a metal-to-insulator transition with clear first-order features or remain metallic down to low temperatures. A simple model consisting of two parallel resistors can be used to quantify a phase coexistence scenario explaining the measured macroscopic transport properties. The interaction between film and substrate is the most plausible candidate to explain this extended phase coexistence, as shown by a correlation between the transport properties and the structural data.

(Some figures in this article are in colour only in the electronic version)

Epitaxial thin films have been the focus of intensive research, owing to their potential applications in emergent technologies and fundamental studies of physical phenomena. In particular, strain introduced by a lattice mismatch between thin film and substrate can be used to alter their properties and stabilize metastable states. An extended temperature regime for phase coexistence has been observed for certain chemical compositions that, in principle, are not allowed by the Gibbs' phase rule [1]. One well documented case is that of perovskite manganite $R_{1-x}A_xMnO_3$ (R = rare earth and A = alkaline earth cations) thin films, which undergo a metal-to-insulator phase transition at a significantly different temperature than those of bulk samples [2]. It should also be noted that the disorder in the ionic radius of the A-site cation has a profound effect on the average ordering temperature of bulk manganites, which often complicates the determination of how much strain contributes to phase separation in thin film samples [3, 4]. Nevertheless, a recent comparison of solid-solution alloy and A-site ordered superlattice $La_{2/3}Ca_{1/3}MnO_3$ thin film samples on different substrates revealed that strain is more important than chemical disorder in stabilizing the mixed phase regime near the average ordering temperature [5]. To investigate further the role of the substrate in the phase separation of a thin film sample, it is interesting to work on a sample which is, in its bulk form, a prototype of a discontinuous transition. In this contribution, the transport properties of epitaxial V_2O_3 thin films are examined.

Vanadium sesquioxide V_2O_3 exhibits a remarkable first-order metal-to-insulator (M–I) transition around 150 K, below which an antiferromagnetic insulating phase exists. Hydrostatic and chemical pressure ($V_{2-x}M_xO_3$ with M = Ti $\cdots$) or sample non-stoichiometry ($V_{2-y}O_3$) significantly lowers this transition temperature [6–9]. In particular, application of hydrostatic pressure above a critical threshold of 26 kbar suppresses the M–I phase transition [10]. Under particular growth conditions, substrate-induced strain also suppresses partially the M–I transition [11, 12], and metallic-like behavior, with some indication of a Fermi liquid regime, is observed below 20 K [11]. The intermediate-temperature regime, which is apparently dependent upon film thickness, is more complex, and a non-monotonic variation of the slope (dR/dT) is observed [13]. Surprisingly, using c-Al_2O_3 [13] or c-$LiTaO_3$ [12], the thicker films present a metallic character. Films thinner than 220 Å recover the M–I transition, although

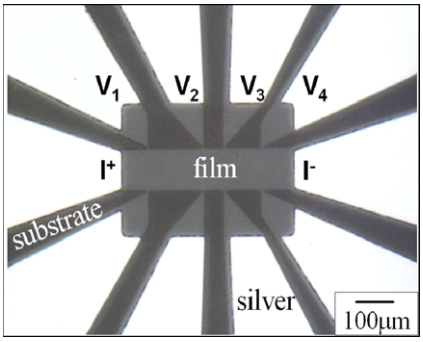

Figure 1. An optical microscopy image of one microbridge patterned (M2, width: 100 μm) for a 230 Å thick V_2O_3 film, where the scale represents 100 μm. The microbridge includes two silver pads for supplying the current (I^+, I^-) and eight silver pads with five different lengths depending on the position of the voltage contacts (V_1, V_2, V_3 and V_4). Our measurements were made between V_1 and V_3, a distance corresponding to 200 μm.

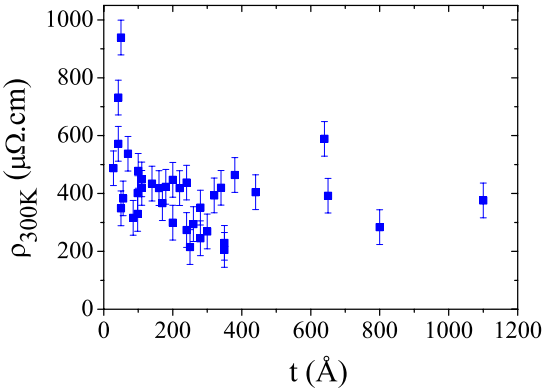

Figure 2. Room temperature resistivity values ($\rho_{300\ K}$) versus the thickness (t) of unpatterned V_2O_3 films.

it is attenuated strongly when compared to the transition observed in the bulk. To clarify such behavior, we have investigated the homogeneity of the samples at the mesoscopic level (where mesoscopic represents a scale below the large statistical collections at which average properties have been measured previously). Using microbridges as local probes, we show in these thin films a phase separation that explains, by using a simple model of two parallel resistors, the evolution of the transport properties at the macroscopic scale. A clear correlation with the structural data is also found.

High quality V_2O_3 films were grown on (0001)-oriented sapphire substrates using the pulsed laser deposition technique. A pulsed KrF excimer laser beam ($\lambda = 248$ nm, pulse length 20 ns, repetition rate 3 Hz) was focused on a V_2O_5 target, depositing films onto the substrate under optimized deposition conditions (650 °C, 0.02 mbar Ar pressure, and a laser fluence of 4 J cm^{-2}). The structure of the resulting films was examined by x-ray diffraction, which attests to their high quality and epitaxial relation with the substrate. The in-depth details of the growth conditions, and some structural and microstructural properties have been reported previously [13]. The resistance of the samples was measured using a physical property measurement system. Electrical transport measurements were made on unpatterned films using a four probe geometry. Silver contact pads, separated by 1 mm, were deposited by thermal evaporation through a mechanical mask. A 230 Å thick sample, which exhibits a low rms roughness of 0.47 nm (averaged over 3 × 3 μm^2), was selected for patterning. A silver layer was deposited onto the film. Contact pads were first defined using ultraviolet (UV) photolithography and chemical etching in a KI/I_2 solution. The V_2O_3 thin film was then patterned by UV photolithography and argon ion etched to form 20 and 100 μm wide bridges. The final microbridge, shown in figure 1, allows for different measurement geometries. For this experiment, the voltage was measured between V_1 and V_3, which corresponds to a length of 200 μm. The external circuitry and the patterned film with silver contact pads were connected using aluminum–silicon wires attached by ultrasonic bonding. Transport measurements were made in 20 × 200 μm^2 (M1) and 100 × 200 μm^2 (M2) bridges. M1 and M2 are located close to each other in the center of the sample. In unpatterned films, we find that the resistivity has an average value of 450 ± 150 $\mu\Omega$ cm at room temperature. In patterned film, we measure 1030 ± 80 $\mu\Omega$ cm for M1 and 950 ± 80 $\mu\Omega$ cm for M2. This increase is almost entirely due to an increase of the residual resistivity. From this we conclude that the patterning process did not significantly alter the film properties and, importantly, that each bridge is nearly identical.

The resistivities of numerous unpatterned V_2O_3 thin films were measured as a function of their thickness (approximately 20 samples with thicknesses t, 40 Å $\leqslant t \leqslant$ 1000 Å). As shown in figure 2, the film resistivities at room temperature are close to 450 ± 150 $\mu\Omega$ cm, values which are similar to the those of the crystals, and do not evolve with the thickness. The resistivity versus temperature curves measured during cooling for samples of different thicknesses are presented in figure 3. While the high-temperature behavior is similar for all the samples, notable differences appear when $T \leqslant 150$ K. Insulating behavior is favored for the thinnest samples and metallic for the thickest. A pure metallic behavior was never observed at the macroscopic scale over the 2–300 K range since a memory of the M–I transition is always observed (even if it is tiny), but metallic behavior is recovered at low temperatures [13]. It should be noted that even the more metallic V_2O_3 behaves as a bad metal and the classical size effect is not observed down to the lowest thickness ($t \approx 42$ Å), which is in agreement with the anomalously low mean free path ($\ell \leqslant 0.2$ nm in a Drude approximation). This explains the thickness independence of the room temperature resistivity. At lower temperatures, the complex behavior of the resistivity requires further investigations. In particular, the resistivity maximum occurring at intermediate temperature may indicate a competition between metallic and insulating states as observed previously in manganites [14]. The phase separation scenario has been used to explain such characteristics and one may ask if the situation is similar in our films. Accordingly, we have performed local resistivity measurements on a sample possessing an intermediate thickness ($t = 230$ Å). This film was selected because it represents the cross-over between the

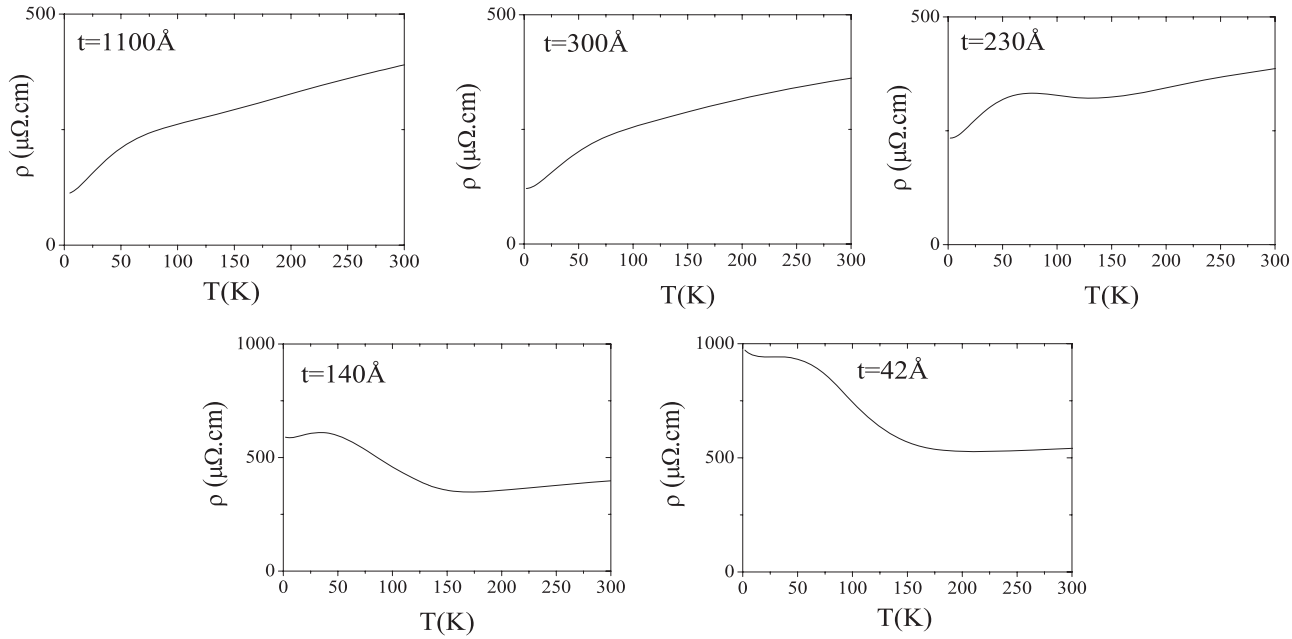

Figure 3. Linear resistivity as a function of the temperature measured during cooling for unpatterned V_2O_3 films of certain thicknesses (noted t).

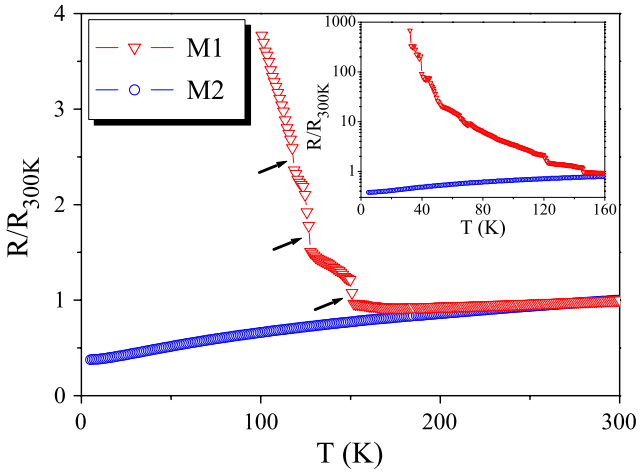

Figure 4. The resistance, normalized over the 300 K value, of a patterned 230 Å thin film of V_2O_3 measured during cooling on two different microbridges (M1: 20 × 200 μm^2, M2: 100 × 200 μm^2). The arrows represent for M1 the different transition temperatures observed. The inset is a close-up near the M–I transition and down to low temperatures.

metallic and the insulating unpatterned film behaviors, and displays a clear maximum in $\rho(T)$ at $T \approx 70$ K. Local resistivity measurements were done using two microbridges (M1 and M2) patterned on this sample in order to observe whether the transport properties are identical at a smaller scale than the macroscopic one. Figure 4 displays the evolution of the resistance ratio $R/R_{300\ \mathrm{K}}$ for each microbridge of this patterned film. From the plots, it is clear that each microbridge exhibits significantly different transport properties for $T \leqslant 150$ K, and that the macroscopic behavior is not simply recovered.

The data for the first microbridge (M1) present a metal-to-insulator transition. While the largest increase in resistance is observed close to 150 K, smaller ones are also observed at certain discrete values: 120 K, 110 K and at approximately each 10 K down to 70 K (as shown on figure 4 by arrows). The transition at 150 K appears similar to the first-order M–I transition observed in pure bulk V_2O_3 samples. The resistance increases by around three orders across the transition between 150 K and the low temperatures, and this is notably less than what is reported for the transition in crystals where the increase can be up to seven orders of magnitude. Since other transitions occur at different temperatures, each jump in resistance can be attributed to the transition of a part of, and not all of, the bridge. Such behavior can explain, at least partially, why the M–I transition is notably attenuated. Owing to the multiple transitions observed, the domain size of one insulating domain is estimated to be smaller than that of the microbridge ($<20 \times 200\ \mu m^2$), but not too small to greatly affect the resistivity, i.e. in the micrometer scale. Two features demonstrate that this transition remains locally first order, even though it is affected by the disorder. Firstly, after cooling the sample, resistance time series were measured at fixed temperatures (figure 5). During these measurements resistance fluctuations were observed, which are large non-Gaussian $1/f^{\alpha}$ noise, and can be attributed to highly inhomogeneous current paths that form when close to an incipient M–I transition [15] or two-state fluctuators. We focus here on the discrete two-state fluctuators near the transition, shown in the inset of figure 5, in the absence of large non-equilibrium noise. The statistics of the two states are largely independent of the applied magnetic field, which demonstrates that the fluctuation of magnetic domains cannot be involved as an origin of this noise (the M–I transition is also a paramagnetic to antiferromagnetic transition, so magnetic effects cannot be completely neglected). Based on work in

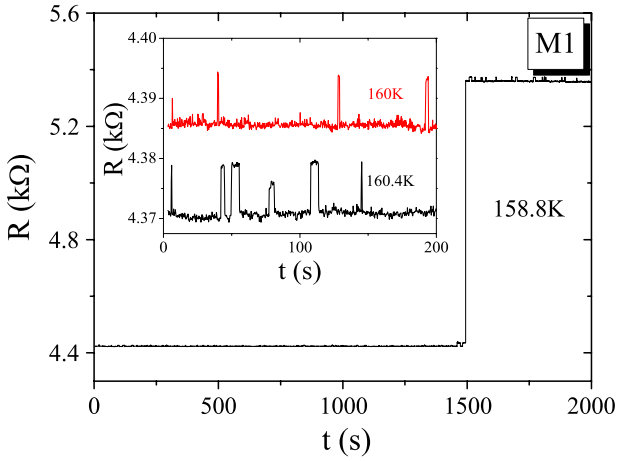

Figure 5. Resistance time series after supercooling for the insulating microbridge M1 of 230 Å thick V_2O_3 film at 158.8 K. The inset shows the resistance fluctuations of two states respectively at 160.4 and 160 K.

colossal magnetoresistive films [16], the measurement of the resistance during long intervals (approximately 1 h for each time series) can be used to extract the main relaxation time τ_i for each state (high resistance ($i = 1$) and low resistance ($i = 2$) states). Assuming $\tau_i \propto \exp(-G_i/K_B T)$ where G_i is the free energy in the state i, the Boltzmann factor $r = \tau_1/\tau_2$ depends on the free energy difference. The latter term then can be used to calculate the entropy difference (ΔS), which we find to be $\Delta S \approx 60 K_B$ using the thermodynamic identity $\Delta S = K_B \partial(T \ln r)/\partial T$. Such behavior is expected when a barrier between two phases exists, and the transition is first-order (rather than second-order) [17]. Secondly, when supercooling from a high temperature, the low resistance state is blocked, and after a certain time the resistance switches suddenly to its high resistance state (see figure 5). This indicates that a metastable state can be supercooled, which is also in agreement with a first-order nature for the transition.

The second curve on figure 4 corresponds to the measurements made on the second microbridge (M2) on the same sample. For this microbridge there is no trace of the M–I transition and the sample behaves as a metal down to 2 K. At low temperature, the resistance follows the expected T^2 temperature variation for electron–electron scattering, as already shown for V_2O_3 thin films and single crystals subjected to high pressures (26–52 kbar) [10, 13]. The detailed analysis of this metallic phase, including magnetoresistance, noise properties, and localization effects will be discussed in another paper. Here, we address whether the suppression of the M–I transition in these domains can be accounted for by substrate-induced pressure. Assuming the film is confined over the surface area of the substrate at the M–I transition temperature leads to an increase of pressure in the film. The maximum effective pressure generated can be estimated [17] using experimental data from bulk samples, such as the stress coefficients C_{11} and C_{12} [19], and the volume change during the bulk M–I transition (we take 2.3% as a representative value, even if some dispersion exists in the literature) [10]. This results in a calculated effective pressure of $(\Delta P) \approx 27$ kbar, and because the decrease in the critical temperature owing to elastic distortion arises from the experimental dP/dT_c [10], the variation in the critical temperature is $(\Delta T_c) \geqslant 160$ K. This value is consistent with the suppression of the M–I transition. Since a first-order transition is heterogeneous when the volume is kept constant because it induces an heterogeneous pressure, such a mechanism will certainly lead to a broad distribution of critical temperatures at a macroscopic scale. As a consequence, for a fixed temperature $T < 150$ K, both metallic and insulating domains with different critical temperatures can coexist.

These results obtained for the microbridges indicate the presence of mesoscopic electronic heterogeneity in V_2O_3 films where metallic and insulating regions coexist over a very large temperature range. Since their properties contrast, clear consequences can be expected for transport properties measured on a large scale, i.e. for unpatterned samples. We suggest that these films consist of different metallic and insulating domains, such as those observed using the microbridges, which are formed below 150 K. In heterogeneous media, percolation theory can be used to calculate the effective resistivity [18], using for example random resistor networks. In the case of large heterogeneities, a coarse-grain approach can be sufficient to give a good description of the resistivity, and the effective resistivity can be described using a parallel-resistor model with a metallic (percolative) resistance and an insulating resistance [14]. We do not have a direct measure of the size of the domains but, as discussed above, we propose that each insulating domain is in the micrometer scale. In the metallic microbridge M2, we do not observe any features (nonlinearities in voltage–current characteristics, thermal hysteresis) which could indicate mixed states at a lower scale, showing that metallic domains are homogeneous over the size of the microbridge or that it is always shorted out by metallic paths, i.e. above the percolation threshold. In phase separated manganites, a coarse-grain approach was strongly guided by the existence of a peak at intermediate temperatures in the effective resistivity, by the large scale (micrometric) of the electronic heterogeneities, and by the recovery of metallic properties at low temperature, indicating that current flows through metallic paths [14, 20, 21]. Here we observe the same characteristics. Consequently, to reconstruct the observed macroscopic behaviors, we also propose a two-parallel-resistors model, with each resistance directly given by the measured resistance in the microbridge (M1 for R_I and M2 for R_M). The ratio of the metallic phase, denoted as x can be used in the following expression to determine the effective conductivity σ,

$$\sigma = x\sigma_M + (1 - x)\sigma_I, \tag{1}$$

where σ_M and σ_I are the conductivity of the metallic and insulating phases of the film, respectively, measured experimentally with the microbridges. The variable in this basic model, except for the x value, is the value of the residual resistivity of the metallic phase, which depends slightly (in a non-trivial way) on the fluctuations of the growth parameters. This variable influences the absolute resistivity value at low

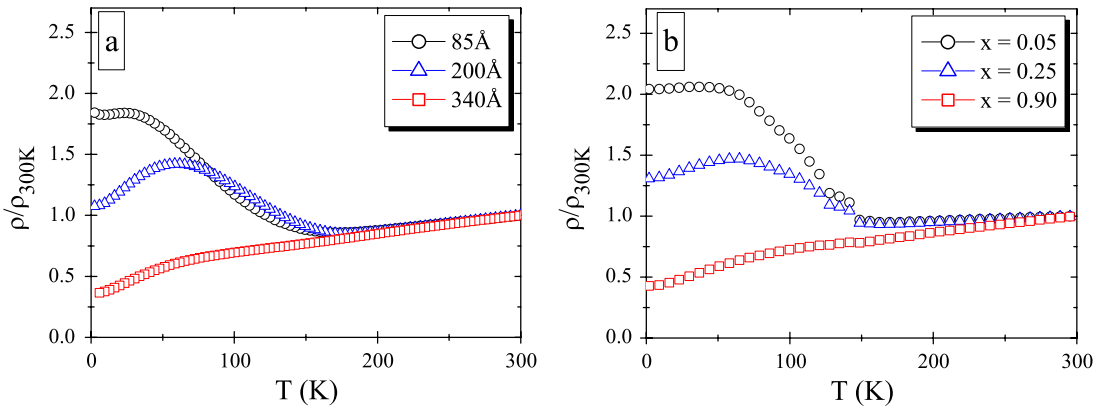

Figure 6. (a) Normalized resistivity ratio $\rho(T)/\rho(300\ \mathrm{K})$ as a function of temperature measured during cooling for three thicknesses. (b) Simulated resistivity ratio ($\rho/\rho_{300\ \mathrm{K}}$) versus temperature for the model of parallel resistances applied to certain metallic ratios x.

temperatures where the current path is essentially in the metallic phase, but, overall, does not significantly alter the functional form of the $R(T)$.

We have applied this phenomenological model to our unpatterned films. Three simulated curves of resistivity as a function of temperature, each corresponding to a different x, are shown in figure 6. The x values, which are temperature independent, were adjusted to match the temperature dependence of simulated curves with those of the experimental curves. The experimental and the calculated curves have very similar appearances, demonstrating that the model (even if simple) is able to explain semi-quantitatively the transport properties. Consequently, the relevant parameter depending on the thickness is the ratio of the conducting phase, x. For each sample, the corresponding x parameter was deduced. Figure 7 shows its thickness dependence, with a large change at a critical thickness $t_c \approx 200$ Å (as shown on the curve by the hatching zone). For $t \geqslant t_c$, x is close to 1, indicating that almost the whole film is metallic. In contrast, for $t < t_c$, x becomes small and the domains with the M–I transition form the majority of the sample, with an electrical behavior similar to the bulk material. The film thickness can therefore be used to control the ratio of the conducting phase and the mesoscopic phase separation. The range of thickness where the phase separation is critical is restricted to the domains of 100 Å $< t <$ 250 Å (see figure 7).

These observations show that the metallic phase in our V_2O_3 films is favored by the large thicknesses. Recalling that metallic V_2O_3 crystals result from an effective applied pressure, we come to the surprising conclusion that the thicker samples are under larger stress than the ultra-thin films.

To explain this unusual evolution of the properties, a structural study was performed. It is known that the ratio of lattice parameters c/a is extremely sensitive to lattice distortions, especially in the case of hexagonal stacking [22, 23]. Figure 8(a) represents the evolution of c/a as a function of the film thickness, deduced from the analysis of x-ray diffraction at room temperature [13]. A small variation in this ratio is observed close to a thickness of 200 Å (indicated by a dotted line in figure 8(a)), which is close to the t_c deduced from the transport properties. Films with $t < t_c$ have a reduced

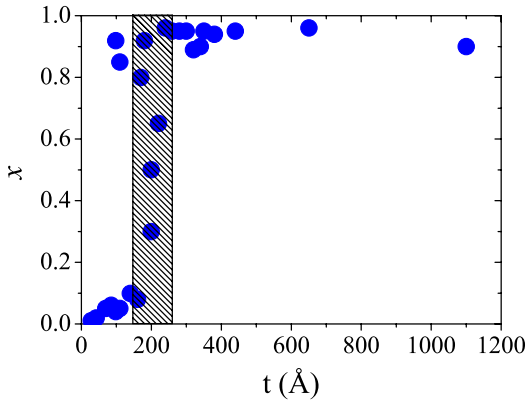

Figure 7. Ratio x of the metallic phase, extracted from the application of the parallel-resistance model, versus thickness of our V_2O_3 films. The hatching zone corresponds to the cross-over thickness, which is close to 200 Å.

ratio c/a (∼2.835), and compare favorably with the value of 2.828 reported for a pure V_2O_3 crystal (dashed line). Films with $t > t_c$ possess a ratio closer to 2.85, the value for a crystal subjected to high hydrostatic pressure (solid line) [22]. A further indication of a structural cross-over at $t \approx t_c$ is observed in figure 8(b). The thick films ($t > t_c$) follow a Poisson law with a calculated Poisson coefficient $\nu \approx 0.5$ (incompressibility limit). In contrast, films with $t < t_c$ do not follow the Poisson law (points surrounded on the curves in figure 8), indicating a change in the elastic properties of the films. Overall, both observations indicate that the thinner films have structural properties close to those of the bulk material, and thus undergo the M–I transition associated with a volume variation.

We have shown that heterogeneous strains induced by the M–I phase change and substrate-induced volume confinement are probably responsible for the broadening of the critical temperature from 150 K until complete suppression for the conducting phase. However, the role of non-stoichiometry, which is known to influence V_2O_3 properties, must also be considered. For $V_{2-y}O_3$ compounds, the ratio c/a remains constant, whatever the y value, and is equal to 2.828 because

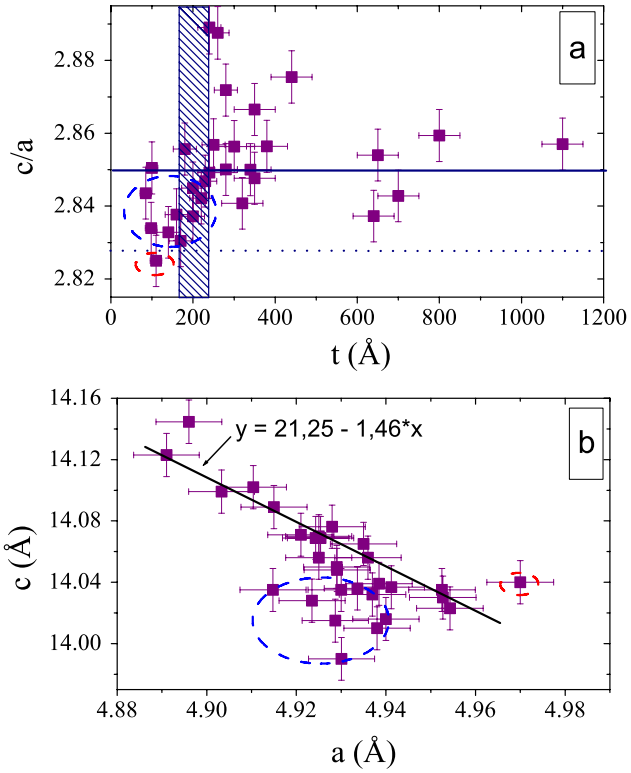

Figure 8. (a) c/a ratio of the lattice parameters versus thickness of V_2O_3 films at room temperature. The hatching zone corresponds to the cross-over thickness, close to 200 Å. The dotted line corresponds to the bulk value, whereas the solid line refers to the value for crystals subjected to a hydrostatic pressure of 47 kbar [22]. (b) Out-of-plane lattice parameter (c) versus in-plane lattice parameter (a) for the different films. The line indicates films following the Poisson law. On both curves, the surrounded points correspond to the same sample thickness ($t < 200$ Å, see the text for details).

both a and c are compressed with respect to stoichiometric V_2O_3 [7]. In our films, c/a varies with t and both a and c exhibit an in-plane compressive lattice parameter and an out-of-plane tensile lattice parameter [13]. In general, the evolution of properties as a function of t in our films cannot be explained by non-stoichiometry, but is consistent with pressure effects [7, 10]. Further studies, including detailed structural studies with transmission electron microscopy, are under way to understand the details of the growth process responsible for the cross-over in the unit cell distortion at $t \approx 200$ Å.

In summary, we have used microbridges as local probes to examine the transport properties of V_2O_3 thin films. Mesoscopic electronic heterogeneities are observed and consist of insulating and metallic zones that coexist over a very large temperature range. This phase separation has a strong influence on the macroscopic transport properties where the evolution of the resistivity as a function of film thickness appears to be governed by the change in quantity of each phase, which is in agreement with the structural data. As in the case of manganite films [17], we believe that such heterogeneous states should be common for films with first-order transitions interacting with a substrate.

This work is carried out in the framework of the STREP CoMePhS (NMP3-CT-2005-517039) supported by the European Commission and by the CNRS, France. W C Sheets was supported additionally by a Chateaubriand postdoctoral fellowship.

References

[1] Kaganer V M, Jenichen B, Schippan F, Braun W, Däweritz L and Ploog K H 2000 *Phys. Rev. Lett.* **85** 341
[2] Prellier W, Lecoeur P and Mercey B 2001 *J. Phys.: Condens. Matter* **13** R915
[3] Moreo A, Yunoki S and Dagotto E 1999 *Science* **283** 2034
[4] Dagotto E, Hotta T and Moreo A 2001 *Phys. Rep.* **344** 1
[5] Palanisami A, Warusawithana M P, Eckstein J N, Weissman M B and Mathur N D 2005 *Phys. Rev.* B **72** 024454
[6] Shivashankar S A and Honig J M 1983 *Phys. Rev.* B **28** 5695
[7] Ueda Y, Kosuge K and Kachi S 1980 *J. Solid State Chem.* **31** 171
[8] McWhan D B, Menth A, Remeika J P, Brinkman W F and Rice T M 1973 *Phys. Rev.* B **7** 1920
[9] Yethiraj M 1990 *J. Solid State Chem.* **88** 53
[10] McWhan D B and Rice T M 1969 *Phys. Rev. Lett.* **22** 887
[11] Autier-Laurent S, Mercey B, Chippaux D, Limelette P and Simon Ch 2006 *Phys. Rev.* B **74** 195109
[12] Allimi B S, Aindow M and Alpay S P 2008 *Appl. Phys. Lett.* **93** 112109
[13] Grygiel C, Simon Ch, Mercey B, Prellier W, Frésard R and Limelette P 2007 *Appl. Phys. Lett.* **91** 262103
[14] Mayr M, Moreo A, Vergés J A, Arispe J, Feiguin A and Dagotto E 2000 *Phys. Rev. Lett.* **86** 135
[15] Seidler G T, Solin S A and Marley A C 1996 *Phys. Rev. Lett.* **76** 3049
[16] Merithew R D, Weissman M B, Hess F M, Spradling P, Nowak E R, O'Donnell J, Eckstein J N, Tokura Y and Tomioka Y 2000 *Phys. Rev. Lett.* **84** 3442
[17] Palanisami A, Merithew R D, Weissman M B, Warusawithana M P, Hess F M and Eckstein J N 2002 *Phys. Rev.* B **66** 092407
[18] Kirkpatrick S 1973 *Rev. Mod. Phys.* **45** 574
[19] Nichols D N, Sladek R J and Harrison H R 1981 *Phys. Rev.* B **24** 3025
[20] de Andrés A, García-Hernández M and Martínez J L 1999 *Phys. Rev.* B **60** 7328
[21] Taran S, Karmakar S, Chatterjee S, Chaudhuri B K, Sun C P, Huang C L and Yang H D 2006 *J. Appl. Phys.* **99** 073703
[22] Finger L W and Hazen R M 1980 *J. Appl. Phys.* **51** 5362
[23] Luo Q, Guo Q and Wang E G 2004 *Appl. Phys. lett.* **84** 2337